

Applying New Laser Interaction Models to the ORION Problem

Claude Phipps^a and John Sinko^b

^a*Photonic Associates, LLC, 200A Ojo de la Vaca Road, Santa Fe NM 87508, USA*

^b*GCOE, Nagoya University, Furo-cho, Nagoya, Aichi, Japan*

Abstract. Previously, Phipps, *et al.* developed a model that permitted laser ablation impulse predictions within a factor of two over an extremely broad range of pulse durations and wavelengths in the plasma regime. This model lacked the ability to predict the intensity for optimum impulse generation. For the lower-intensity vapor regime, below the plasma transition, Sinko developed a useful, fluence-dependent model which predicts impulse delivered for pulsed lasers on polymers at a specific wavelength. Phipps subsequently developed an alternate model which treats elemental solids in the vapor regime, that only requires knowledge of basic material parameters and vapor pressure vs. temperature data. These data, except for optical absorptivity, are wavelength-independent. A simple technique combines either vapor model with the plasma model to form a complete model that moves smoothly through the vapor to plasma transition. In this paper, we apply these models to show the optimum momentum coupling fluence on target, at the transition from the vapor to the plasma regimes, for aluminum (a typical debris material) and polyoxymethylene (representing polymeric debris). The application of this work is the ORION laser space debris mitigation concept. This is an improvement over previous work, in which this optimum was only estimated from the plasma ignition threshold. We present calculations showing how impulse delivered to debris targets in the ORION concept varies with pulse duration, at an optimum fluence determined by nonlinear optical effects in the Earth's atmosphere.

Keywords: ORION, space debris, laser materials interaction, impulse coupling

PACS: 52.38.Mf, 79.20.Eb, 41.75.Jv

THE NEAR-EARTH SPACE DEBRIS PROBLEM

One result of 35 years of space activity is that there are now several hundred thousand pieces of space debris larger than 1cm in near-Earth orbit. Debris in the 1-10-cm size range are especially hazardous to near-Earth space assets because they are not tracked, but can cause fatal damage. Larger objects can usually be tracked and avoided (although this is becoming more difficult with time), while spacecraft shielding is practical for smaller objects. The 1 – 10-cm debris were created from explosions or mutual collisions and, because of the range of launch latitudes and inclinations of the source objects, their typical velocity in the reference frame of an orbiting spacecraft is 12km/s. Their density maximizes in the 400- to 1100 km altitude range.

The debris problem has become more urgent recently. In February 2009, an American communications satellite collided with a Russian Kosmos satellite, spreading debris around the Earth and prompting concerns about the safety of the final

Hubble service mission. In March, 2009, the International Space Station crew spent the morning taking cover in a Soyuz capsule to reduce their cross-section in the event of collision with a space debris object whose track might have intercepted the Space Station. Mutual collisions will continue to increase the debris density until the problem is dealt with.

The concept of removing the debris with a high-power, pulsed, ground-based laser system was first presented in 1993 [1]. Laser space debris removal uses a high-intensity pulsed laser beam to ablate (not pulverize) a fraction of the debris itself in an orientation such that the debris is slowed sufficiently to re-enter the atmosphere and burn up. Pulsed lasers are much more effective for this purpose than CW lasers, because the latter tend to melt the target and create more debris.

The concept was later named ORION by NASA headquarters staff, who authorized a concept validation study in 1995 [2, 3]. The study concluded that the capability to remove essentially all dangerous orbital debris in the 1 – 10-cm range between 400 and 1100 km altitude was feasible within two years, and that its cost would be modest relative to the likely costs to shield, repair, or replace high-value spacecraft that could otherwise be lost to debris impacts.

INTRODUCTION: LASER ABLATION IMPULSE MODELS

When a laser pulse is incident on a target in vacuum, mechanical impulse is produced by the pressure of photoablation at the target surface. The figure of merit for this interaction with pulsed laser intensity I is the mechanical coupling coefficient C_m , conventionally expressed in mixed units as:

$$C_m = p/I \text{ dyn/W} \quad (1)$$

where p is the ablation pressure in dyn/cm². Since typical C_m values are of order 1 – 10, the portion due to light pressure ($C_{hv} = 2/c = 6.7E-4 \text{ dyn/W}$) is relatively ignorable.

Because of its crucial importance to the design of laser space propulsion engines in general, as well as to ORION [4], it is important to be able to predict how C_m will vary with laser pulse intensity I , wavelength λ and pulse duration τ for a given material in vacuum. Even more important is the ability to predict at what intensity the maximum C_m is found, and this requires knowing how to combine vapor and plasma ablation models.

As intensity is increased, the ablation process begins in the vapor regime and progresses to the fully-formed plasma regime where the ionization fraction

$$\eta_i = n_i/(n_o + n_i) \approx 1, \quad (2)$$

(n_i is the ion number density) and the optical spectrum and heat flux transferred to the target surface is entirely mediated by the plasma layer. For intensities above this transition, C_m is progressively reduced. Phipps, *et al.* [5] developed a model that permitted laser ablation impulse predictions within a factor of two over an extremely broad range of pulse durations and wavelengths in the plasma regime, but it lacked the

ability to predict the intensity for optimum C_m . Since this is a physically complex transition, treatments prior to [6] treated the vapor and plasma regimes separately, and no means was provided to predict C_m through the transition. Model [6] treated this transition well for single polymers where ablation thresholds Φ_0 are well-defined. However, predictions were limited to a single wavelength and pulse duration, since Φ_0 is wavelength dependent, because it involves Φ_0 explicitly, and is usually dependent on pulse duration as well.

On the other hand, for elemental surface absorbers such as Al, for which p(T) tables such as the SESAME tables exist, a different approach which is somewhat more general can be used to advantage [7].

In this paper, we apply both approaches to the calculation of debris velocity changes in the ORION application, for polymers and for aluminum debris, respectively. We restrict consideration to the range $100\text{ps} < \tau < 1\text{ms}$ and $248\text{nm} < \lambda < 10.6\mu\text{m}$ and intensities expressed as $I\lambda^2 < 1\text{E}6 \text{ W}$ (i.e., below the inertially confined fusion regime treated by Lindl [8]). We do not treat effects in atmosphere here, nor CW laser irradiation, which is the subject of a subsequent paper.

Plasma Regime

In the plasma regime defined by Eq. (2), it was shown by Phipps, *et al.* [5] that the simple relationship

$$C_{mp} = 5.83 \frac{\Psi^{9/16}}{A^{1/8} (I \lambda \sqrt{\tau})^{1/4}} \quad \text{dyn/W} \quad (3)$$

describes C_m to within a factor of two for surface absorbers in the plasma-dominated regime. There also resulted

$$I_{sp p} = 1400 \frac{A^{1/8}}{\Psi^{9/16}} (I \lambda \sqrt{\tau})^{1/4} \quad \text{s} \quad (4)$$

for the plume “specific impulse,” v_{plume}/g_0 . In Eq. (3),

$$\Psi = \frac{A}{2[Z^2(Z+1)]^{1/3}}, \quad (5)$$

where A is the average atomic mass number and $Z \geq 1$ is the average ionization state in the laser-produced plasma plume, which is, in turn, determined by applying Saha’s equation [9],

$$\frac{n_e n_j}{n_{j-1}} = \frac{2u_j}{u_{j-1}} \left(\frac{2\pi A m_p k T_e}{h^2} \right)^{3/2} \exp(-W_{j,j-1}/kT_e), \quad (6)$$

and writing

$$Z = n_e/n_i, \quad (7)$$

under the obvious normalization constraint

$$\sum_{j=1}^{j_{\max}} (n_j) = n_i \quad (8)$$

Parameters in the preceding relationships are: $W_{j, j-1}$, the ionization energy difference between the (j-1)th and jth ionization states of the material; m_e , the electron mass; kT_e , the electron temperature in the plasma plume (eV); Planck's constant h ; the neutral vapor density n_o ; c , the speed of light; I the incident laser intensity (W cm^{-2}); the plume electron total number density n_e (cm^{-3}); u_j the quantum-mechanical partition functions of the jth state; and n_j , the number density of each of the ionized states.

Polymers in the Vapor Regime

The Sinko/Phipps vapor model [6] applies best to polymers, where tables of vapor pressure vs. temperature $p(T)$ are difficult or impossible to obtain, but where the fluence for onset of ablation Φ_o is well known. Because Φ_o usually depends on wavelength and pulse duration, this approach is best applied to one combination of (λ, τ) at a time, but works very well. Where

$$\mu = (\rho/\alpha)\ln(C\Phi/\Phi_o) \quad (9)$$

is the ablated mass areal density and C is a constant combining energy losses such as reflectivity and exhaust energetic modes that do not contribute to propulsion, which is equal to the ablation efficiency, the ablation momentum areal density σ can be related to the laser parameters by energy conservation:

$$\sigma^2/2\mu = C\Phi - \Phi_o = \Phi_o (\xi-1), \quad (10)$$

(where $\xi = C\Phi/\Phi_o$). Based on Eq. (9 – 10), the momentum coupling coefficient and specific impulse can be obtained as

$$C_{mv} = \sigma/\Phi = \sqrt{\frac{2\rho C^2(\xi-1)\ln\xi}{\alpha\Phi_o\xi^2}} \quad (11)$$

$$I_{spv} = \sqrt{\frac{2\alpha\Phi_o(\xi-1)}{\rho g_o^2 \ln\xi}} \quad (12)$$

Elemental Materials in the Vapor Regime

For some elemental materials, tables of vapor pressure vs. temperature $p(T)$ exist, e.g., the Los Alamos SESAME tables [10]. For such materials, by working backwards from hydrodynamic variables based on wavelength-independent material parameters to the incident intensity I which must exist to balance these variables, we showed in [7] that the expressions

$$I = \frac{pv}{a} \left(\frac{\gamma}{\gamma-1} \right) \left[1 - \frac{T_o}{T} + \frac{q}{C_p T} + \frac{\gamma-1}{2} \right] + \frac{\sigma \varepsilon}{a} T^4 + B(\tau) \quad (13)$$

where

$$B(\tau) = \frac{1}{a} \left[\phi(T, x_h) + \frac{x_h \rho_s C_v (T - T_o)}{\tau} \right] \quad (14)$$

can be used to generate a numerical solution which relates ablation pressure p and vapor velocity v to I over the range corresponding to our $p(T)$ data, and we can compute the vapor regime coupling coefficient (for elemental materials such as aluminum) as

$$C_{mv} = p/I \quad (15)$$

Vapor specific impulse is

$$I_{spv} = v/g_o \quad (16)$$

These relationships are wavelength-independent, except for the variation of a with λ .

Combined Models

Having results for the two physical extremes of vapor and plasma, we make a smooth transition between the models using the approach of [6], writing for the combined coupling coefficient,

$$C_m = p/I = [(1-\eta_i)p_v + \eta_i p_p]/I = (1-\eta_i) C_{mv} + \eta_i C_{mp} \quad (17)$$

where the ionization fraction η_i [Eq. (2)] is determined during the process indicated in Eqs. (6-8). Specific impulse can be combined in the same way. Figures 1 and 2 show the success of these approaches for typical polymer (polyoxymethylene) and a typical elemental material (aluminum) which are representative of materials of interest in the ORION debris reduction program.

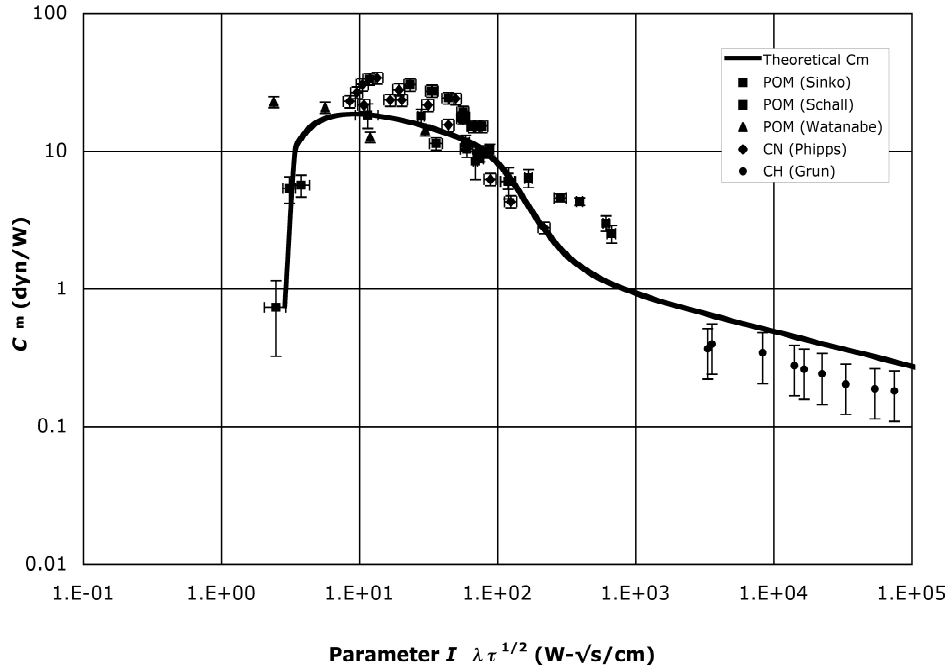


FIGURE 1. The Sinko/Phipps polymer model model fits data well from ablation threshold up to inertial confinement fusion conditions. References are given in [6].

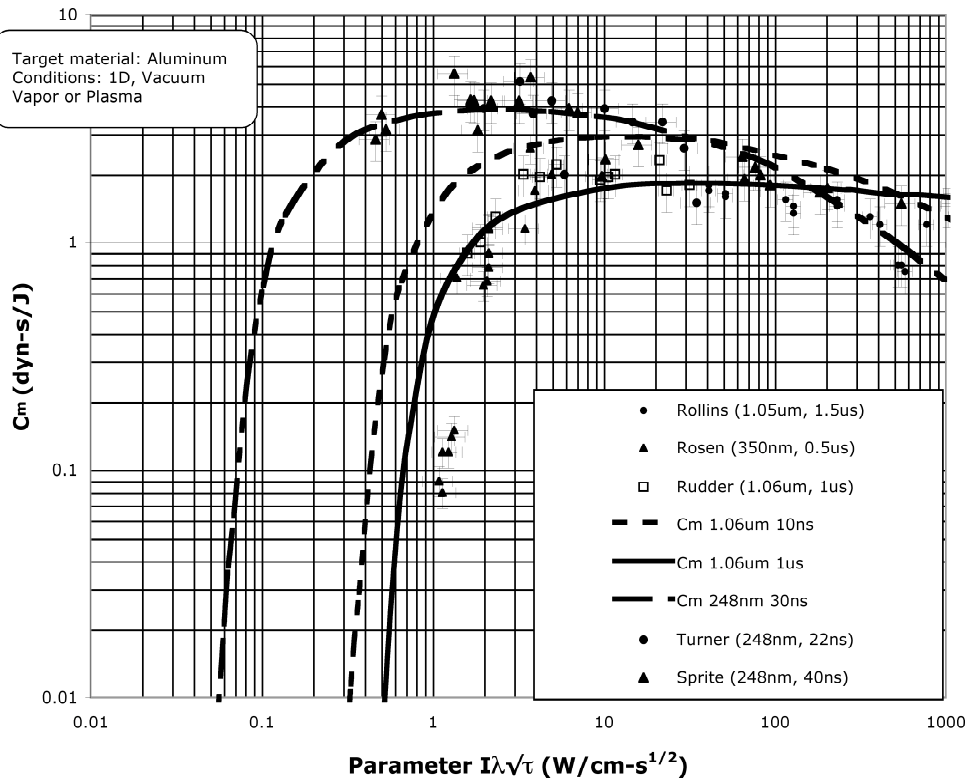


FIGURE 2. Fitting mechanical coupling data for Nd laser wavelengths with the combined model for aluminum. Rollins and Rudder references are given in [7]. The 10ns model and the 248nm data and fit are included to show the effects of pulsewidth and wavelength on model predictions.

In the following, these data will be used to estimate Δv applied to specific space debris in the ORION application.

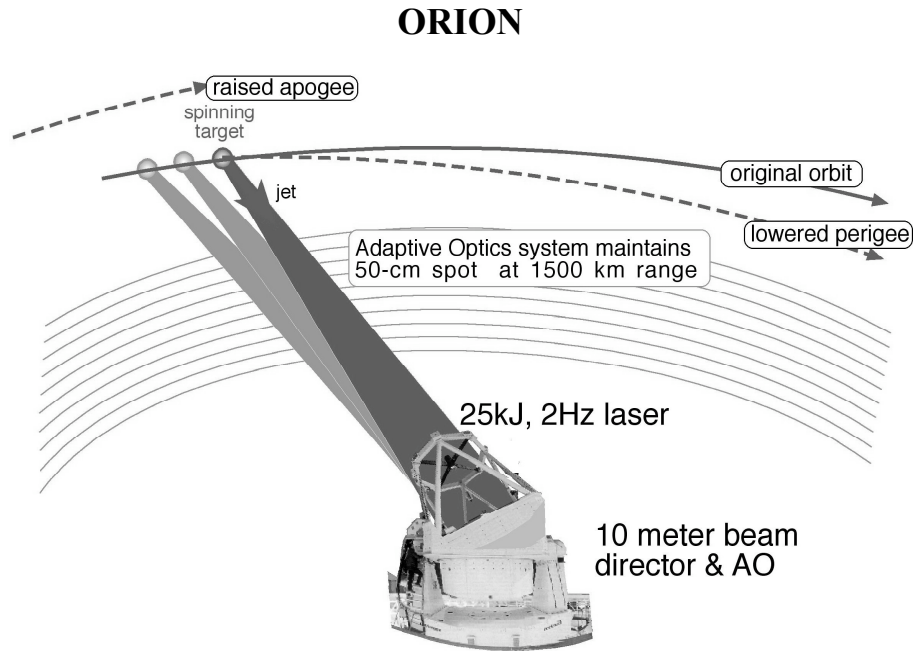


FIGURE 3. The ORION concept.

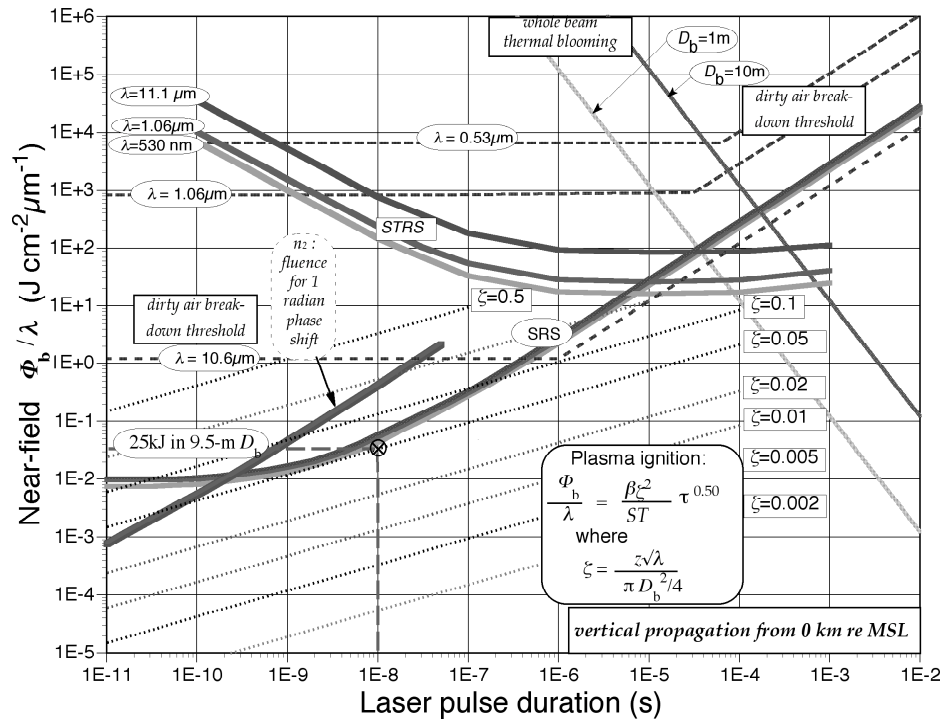


FIGURE 4. The ORION propagation chart. Beam fluence in the atmosphere is set by plasma ignition requirements on a distant target. Strehl ratio $S = 0.25$, atmospheric transmission $T = 0.85$ and $\lambda = 1.06 \mu\text{m}$.

In the Figure the fluence on target is set to

$$\Phi = \beta \tau^{1/2} \quad \text{J/cm}^2 \quad (14)$$

as an approximation to the peak fluence in Figs. (1) and (2). Beam fluence in the atmosphere is constrained above and below. Where z is target range, λ is wavelength D_b is launching aperture diameter, and ξ incorporates the effects of diffraction, the minimum fluence is expressed as

$$\frac{\Phi_b}{\lambda} \geq \frac{\beta \xi^2 \sqrt{\tau}}{S T} \quad (15)$$

while maximum fluence is set by nonlinear optical effects in the atmosphere including (for short pulses) phase distortions due to nonlinear index (n_2) and stimulated rotational Raman scattering (SRS). Details of the calculations on which Figure 4 is based are provided in [3]. In the Figure, an operating point is shown corresponding to beam pulse energy 76kJ above the atmosphere (89 kJ on the ground) arising from a 9.5-m-diameter mirror. For the $\tau = 100$ ns pulse in the example, fluence on a target at range 1500km is 29.8 J/cm². The spot size on target $d_s = 57$ cm.

Velocity change per pulse is given by the relationship

$$\Delta v = \Phi C_m / \mu \quad (16)$$

where μ is the target mass density in g/cm², and it is assumed in Tables 1 and 2 that the target is no larger than the beam diameter at range z . $\langle P \rangle$ is laser average power (repetition frequency times pulse energy) for target re-entry in a single pass lasting 67 seconds. Wavelength $\lambda = 1.06\mu\text{m}$ is assumed. It is highly desirable to cause re-entry of the 1 – 10-cm targets in one pass overhead the ORION laser site, because this permits us to forego subsequent tracking for these difficult-to-detect objects. The Tables assume achievement of this goal. In Table 2, we assume that C_m is as given in Figure 1 although that data is for 10.6 μm .

TABLE 1. Interaction Parameters for $\mu = 0.5\text{g/cm}^2$ Aluminum Targets ($d_s = 57\text{--}60$ cm at 1500km) at 1.06 μm wavelength

Pulse Duration τ (ns)	C_m peak (dyn/W)	$I\lambda\sqrt{\tau}$ peak (W/cm-s ^{1/2})	Mirror Diameter D_b (cm)	Laser Pulse Energy (kJ)	Fluence on Target (J/cm ²)	Freq. f (Hz)	Δv per pulse (cm/s)	$\langle P \rangle$ (kW)
0.1	3.0	3.8	900	1.2	0.36	105	2.1	125
1	2.7	10	950	8.9	3.0	14	17	121
10	3.0	10	950	28	9.4	4.0	57	112
100	2.0	30	950	140	90	0.63	360	168

TABLE 2. Interaction Parameters for $\mu = 0.5\text{g/cm}^2$ Delrin Targets ($d_s = 57\text{--}60$ cm at 1500km)

Pulse Duration τ (ns)	C_m peak (dyn/W)	$I\lambda\sqrt{\tau}$ peak (W/cm-s ^{1/2})	Mirror Diameter D_b (cm)	Laser Pulse Energy (kJ)	Fluence on Target (J/cm ²)	Freq. f (Hz)	Δv per pulse (cm/s)	$\langle P \rangle$ (kW)
100	20	10	750	140	30	0.19	1200	26

With a one minute retargeting interval and a 67 second interaction interval, 680 objects of the sort listed in Tables 1 and 2 can be re-entered per day, and 250k objects per year. The mass of the objects is 1.7 kg or less. However, much heavier objects up to one tonne could be re-entered in ten months after multiple passes by a laser station with 280 kW time-average power, given 5 minutes interaction time in two weeks.

DEBRIS REMOVAL STRATEGY

There are about $N_1 = 6,000$ large objects (diameter $> 100\text{cm}$) in low Earth orbit, and $N_2 = 300\text{k}$ small objects (diameter $> 1\text{cm}$). The collision rates for the large ones are about $R_1 = 7.0\text{E-}7 \text{ m}^{-2}\text{year}^{-1}$ and $R_2 = 3.7\text{E-}5\text{m}^{-2}\text{year}^{-1}$ for the small ones [11]. Assuming the large objects have $\sigma = 5\text{m}^2$ cross-sectional area, the interval between collisions of type i on the large ones across the ensemble

$$T_{i1} = [\sigma N_1 R_i]^{-1} \quad (17)$$

Applying Eq. (17), we estimate that the chance that a big object will destroy a big object is once in 50 years, whereas the chance a small object will destroy a big object is once in 10 months. This is why a system that can address the small objects is important.

DISCUSSION

Even though a 140kJ/pulse laser operating at 12 pulses per minute might is not yet within the state of the art, we believe it will be soon. The average power is much more reasonable than for the other combinations of parameters. Table 2 indicates a clear advantage for propelling polymer debris targets. The beam director diameter, set by the combination of nonlinear optical effects in the atmosphere and the achievement of the correct target fluence for maximum coupling, is significantly smaller than for the Table 2 case than for the other cases. Addressing only large debris objects was shown not to be the best strategy, based on published debris statistics, and it requires lasers which are even further beyond the state of the art. Using cost estimation methods reported in [3], we can estimate that the small objects can be removed at a cost of \$330 each, including supplies and personnel, with system costs amortized over three years.

ACKNOWLEDGMENTS

This work was supported by Photonic Associates, LLC's internal research and development fund. We gratefully acknowledge the assistance of Dr. Kevin Honnell, Los Alamos National Laboratory, with the SESAME database.

REFERENCES

1. C. R. Phipps, "A laser concept for clearing space junk," in *AIP Conference Proceedings* **318**, Laser Interaction and Related Plasma Phenomena, 11th International Workshop, Monterey, CA October, 1993, George Miley, ed. American Institute of Physics, New York (1994)pp. 466-8
2. C. R. Phipps, H. Friedman, D. Gavel, J. Murray, G. Albrecht, E. V. George, C. Ho, W. Priedhorsky, M. M. Michaelis and J. P. Reilly, "ORION: Clearing near-Earth space debris using a 20-kW, 530-nm, Earth-based, repetitively pulsed laser", *Laser and Particle Beams*, **14** (1) (1996) pp. 1-44
3. C. R. Phipps in *Project ORION: Orbital Debris Removal Using Ground-Based Sensors and Lasers*, J. W. Campbell, ed. NASA Marshall Spaceflight Center Technical Memorandum 108522 October 1996
4. C. Phipps, M. Birkan, W. Bohn, H.-A. Eckel, H. Horisawa, T. Lippert, M. Michaelis, Y. Rezunkov, A. Sasoh, W. Schall, S. Scharring and J. Sinko, "Laser Ablation Propulsion," *J. Propulsion and Power*, to appear (2010)
5. C. R. Phipps, Jr., T. P. Turner, R. F. Harrison, G. W. York, W. Z. Osborne, G. K. Anderson, X. F. Corlis, L. C. Haynes, H. S. Steele, K. C. Spicochi and T. R. King, "Impulse Coupling to Targets in Vacuum by KrF, HF and CO₂ Lasers", *J. Appl. Phys.*, **64**, 1083 (1988).
6. J. Sinko and C. Phipps, "Modeling CO₂ laser ablation impulse of polymers in vapor and plasma regimes," *Appl. Phys. Lett.*, **95**, 131105-1 to 131105-3 (2009)
7. C. Phipps, "An Alternate Treatment of the Vapor-Plasma Transition," *Int. J. Aerospace Innovations* **1**(1) to appear (2010)
8. J. Lindl, *Phys. Plasmas*, **2**, 3933 (1995)
9. M. Saha, "Ionization in the solar chromosphere," *Phil. Mag.* **40**, 472 (1920)
10. The SESAME equation-of-state database is maintained by group T-1 at Los Alamos National Laboratory (sesame@lanl.gov); see S.P. Lyon and J.D. Johnson, "SESAME: The Los Alamos National Laboratory Equation of State Database," LANL Report No. LA-UR-92-3407 (1992) for additional information.
11. H. Klinkrad, *Space Debris – Models and Risk Analysis*, Springer/Praxis 2006, p. 126